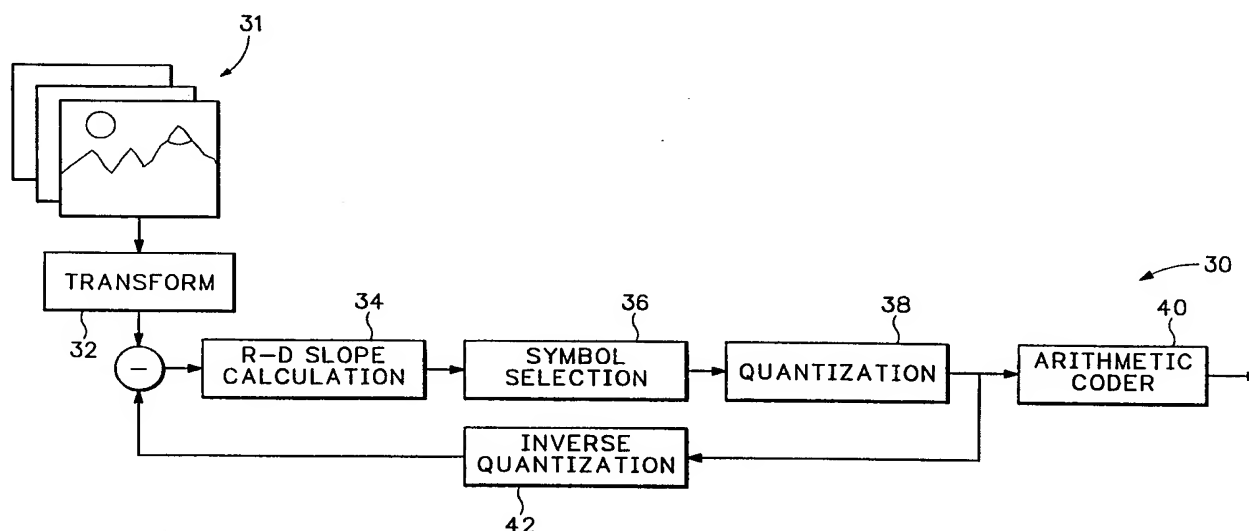




INTERNATIONAL APPLICATION PUBLISHED UNDER THE PATENT COOPERATION TREATY (PCT)

| | | |
|--|-----------|---|
| (51) International Patent Classification ⁶ : G06K 9/36, 9/46 | A3 | (11) International Publication Number: WO 98/34398 (43) International Publication Date: 6 August 1998 (06.08.98) |
| (21) International Application Number: PCT/US98/01981 (22) International Filing Date: 30 January 1998 (30.01.98) (30) Priority Data: 60/035,126 3 February 1997 (03.02.97) US Not furnished 30 January 1998 (30.01.98) US (71) Applicant: SHARP LABORATORIES OF AMERICA, INC. [US/US]; 5750 N.W. Pacific Rim Boulevard, Camas, WA 98607 (US). (72) Inventors: LI, Jin; 900 S.E. Park Crest Avenue #R197, Vancouver, WA 98683 (US). LEI, Shaw-Min; 4522 N.W. Valley Street, Camas, WA 98607 (US). (74) Agents: FORD, Stephen, S. et al.; Marger, Johnson, McCollom & Stolowitz, P.C., 1030 S.W. Morrison Street, Portland, OR 97205 (US). | | (81) Designated States: CN, JP, KR, SG, European patent (AT, BE, CH, DE, DK, ES, FI, FR, GB, GR, IE, IT, LU, MC, NL, PT, SE). Published <i>With international search report.</i> <i>Before the expiration of the time limit for amending the claims and to be republished in the event of the receipt of amendments.</i> (88) Date of publication of the international search report: 26 November 1998 (26.11.98) |

(54) Title: AN EMBEDDED IMAGE CODER WITH RATE-DISTORTION OPTIMIZATION

**(57) Abstract**

A rate-distortion optimized embedding (RDE) coder (Fig. 5) optimizes rate-distortion performance by coding information bits in the order of their R-D slope. RDE allocates the available coding bits first to the information bit with the steepest R-D slope (fig. 9), which indicates the largest distortion decrease per coding bit. The resultant RDE bitstream can be truncated at any point and still maintain an optimal R-D performance. To avoid the overhead of coding order transmission, an expected R-D slope is calculated by both the encoder and the decoder from previous RDE coded bits. A probability estimation table from a QM arithmetic coder (fig. 5, code 40) allows the R-D slope to be derived using a lookup table operation. The rate-distortion optimized embedding (RDE) coder significantly improves the coding efficiency over a wide range of bit rates.

FOR THE PURPOSES OF INFORMATION ONLY

Codes used to identify States party to the PCT on the front pages of pamphlets publishing international applications under the PCT.

| | | | | | | | |
|----|--------------------------|----|--|----|--|----|--------------------------|
| AL | Albania | ES | Spain | LS | Lesotho | SI | Slovenia |
| AM | Armenia | FI | Finland | LT | Lithuania | SK | Slovakia |
| AT | Austria | FR | France | LU | Luxembourg | SN | Senegal |
| AU | Australia | GA | Gabon | LV | Latvia | SZ | Swaziland |
| AZ | Azerbaijan | GB | United Kingdom | MC | Monaco | TD | Chad |
| BA | Bosnia and Herzegovina | GE | Georgia | MD | Republic of Moldova | TG | Togo |
| BB | Barbados | GH | Ghana | MG | Madagascar | TJ | Tajikistan |
| BE | Belgium | GN | Guinea | MK | The former Yugoslav Republic of Macedonia | TM | Turkmenistan |
| BF | Burkina Faso | GR | Greece | | | TR | Turkey |
| BG | Bulgaria | HU | Hungary | ML | Mali | TT | Trinidad and Tobago |
| BJ | Benin | IE | Ireland | MN | Mongolia | UA | Ukraine |
| BR | Brazil | IL | Israel | MR | Mauritania | UG | Uganda |
| BY | Belarus | IS | Iceland | MW | Malawi | US | United States of America |
| CA | Canada | IT | Italy | MX | Mexico | UZ | Uzbekistan |
| CF | Central African Republic | JP | Japan | NE | Niger | VN | Viet Nam |
| CG | Congo | KE | Kenya | NL | Netherlands | YU | Yugoslavia |
| CH | Switzerland | KG | Kyrgyzstan | NO | Norway | ZW | Zimbabwe |
| CI | Côte d'Ivoire | KP | Democratic People's Republic of Korea | NZ | New Zealand | | |
| CM | Cameroon | KR | Republic of Korea | PL | Poland | | |
| CN | China | KZ | Kazakhstan | PT | Portugal | | |
| CU | Cuba | LC | Saint Lucia | RO | Romania | | |
| CZ | Czech Republic | LI | Liechtenstein | RU | Russian Federation | | |
| DE | Germany | LK | Sri Lanka | SD | Sudan | | |
| DK | Denmark | LR | Liberia | SE | Sweden | | |
| EE | Estonia | | | SG | Singapore | | |

AN EMBEDDED IMAGE CODER WITH RATE-DISTORTION OPTIMIZATION

BACKGROUND OF THE INVENTION

5 This invention relates to embedded coding techniques and more particularly to an embedded image coder with improved rate-distortion.

Embedded image coding improves coding performance and also allows a bitstream to be truncated at any point and still decode a reasonably good image. Some representative embedded coding techniques include the embedded zerotree wavelet coding (EZW) discussed in J. Shapiro, "Embedded image coding using zerotree of wavelet
10 coefficients", IEEE Trans. On Signal Processing, vol. 41, pp.3445-3462, Dec. 1993, the set partitioning in hierarchical trees (SPIHT) discussed in A. Said, and W. Pearlman, "A new, fast and efficient image codec based on set partitioning in hierarchical trees", IEEE Trans. On Circuit and System for Video Technology, Vol. 6, No. 3, Jun. 1996, pp. 243-250 and
15 the layered zero coding (LZC) discussed in, D Taubman and A. Zakhor, "Multirate 3-D subband coding of video", IEEE Trans. On Image Processing, Vol. 3, No. 5, Sept. 1994, pp.572-588.

The ability to adjust the compression ratio by simply truncating the coding bitstream makes embedding attractive for a number of applications such as progressive image
20 transmission, internet browsing, scalable image and video databases, digital cameras, low delay image communications, etc. Taking internet image browsing as an example, embedded coding requires storage on a server of only one copy of a high quality image. Depending on user demand, channel bandwidth conditions, and browser monitor quality, selectable amounts of the image bit stream can be delivered to the browser. At an early
25 stage of browsing, images can be retrieved with coarse quality so that a user can quickly go through a large number of images before choosing one image of interest. The chosen image can then be fully downloaded with a better quality level. During the download process, the image quality is gradually refined. The user can terminate the download process as soon as the quality is satisfactory to discern the image.

30 Embedded coding allows the bitstream to be arbitrarily truncated. However, existing embedded coding techniques are not optimized at every truncation point in the bit stream. Thus, if the encoded bitstream is truncated at random points in the bit stream, the

image produced by the bit stream up to the point of truncation does not necessarily produce optimal image quality.

It is known that a fixed rate coder achieves optimality if the rate-distortion (R-D) slopes of all coded coefficients are the same, T. M. Cover and J. A. Thomas, "Elements of information theory", Chapter 13, John Wiley & Sons Inc, 1991. The criterion was used in rate control to adjust the quantization step size Q of each macroblocks, in which case the coding of video was optimal when the R-D slopes of all macroblocks were constant. See L.-J. Lin, A. Ortega and C.-C. J. Kuo, "Rate control using spline-interpolated R-D characteristics", SPIE: Visual Communication and Image Processing, vol. 2727, Orlando, FL, Apr. 1996, pp. 111-122 and K. Ramchandran, A. Ortega and M. Vetterli, "Bit allocation for dependent quantization with applications to multiresolution and MPEG video coders", IEEE Trans. On Image Processing, Vol. 3, No. 5, Sep. 1994, pp. 533-545.

Xiong and Ramchandran use the constant rate-distortion slope criterion to derive the optimal quantization for wavelet packet coding. Z. Xiong and K. Ramchandran, "Wavelet packet-based image coding using joint space-frequency quantization", First IEEE International Conference on Image Processing, Austin, Texas, Nov. 13-16, 1994. However, Xiong and Ramchandran do not optimize rate-distortion optimization for embedded coders.

The R-D slopes of significance identification and refinement coding are different, and by placing the significance identification before the refinement coding, the coding efficiency can be improved. However, the improvement is limited since only the coding order of a few coefficients is effected. See Li, Cheng and Kuo J. Li, P. Cheng and C. -C. J. Kuo, "On the improvements of embedded zerotree wavelet (EZW) coding", SPIE: Visual Communication and Image Processing, vol. 2601, Taipei, Taiwan, May. 1995, pp. 1490-1501.

Thus, a need remains for an embedded coder that optimizes rate-distortion at many different truncation points in an encoded bit stream.

SUMMARY OF THE INVENTION

A rate-distortion optimised embedding (RDE) coder optimises rate-distortion performance by coding coefficients in order of their R-D slope. RDE allocates the available coding bits first to the coefficient with the steepest R-D slope, which indicates

the largest distortion decrease per coding bit. The resultant RDE bitstream can be truncated at any point and still maintain an optimal R-D performance. To avoid the overhead of coding order transmission, an expected R-D slope is calculated by both the encoder and the decoder from previous RDE coded bits. A probability estimation table from a QM arithmetic coder allows the R-D slope to be derived using a lookup table operation. The RDE rate-distortion optimisation significantly improves the coding efficiency over a wide bit rate range.

The RDE embedded coding method digitizes the image and then transforms the image to form a set of coefficients each comprising multiple bits. The RDE coder repeatedly analyzes all the candidate bits before encoding individual bits. The candidate bits comprise one most significant unencoded bit from each coefficient. Individual rate-distortion values for the candidate bits represent a ratio of information content in the bit per cost in transmitting the bit. Selected bits are then encoded according to the associated distortion reduction values for the bits.

In one embodiment, one bit among the candidate bits having a maximum distortion reduction value is encoded. The candidate bits are updated comprising a next less significant bit in the encoded bit coefficient and the remaining unencoded candidate bits. The bit among the candidate bits with the highest distortion reduction value per coding bit is encoded next. The process is repeated until the RDE coder reaches a specified bit rate.

In another embodiment, a threshold value is set and the candidate bits having distortion reduction values greater than the threshold are encoded in each scan. The candidate bits are updated comprising a next less significant bit in the encoded bit coefficient and the remaining unencoded candidate bits. The threshold value is then reduced and a next set of unencoded candidate bits are processed. The candidate bits in the next set having distortion reduction values greater than the reduced threshold value are then encoded. The process is repeated until the RDE coder reaches the predetermined bit rate.

The foregoing and other objects, features and advantages of the invention will become more readily apparent from the following detailed description of a preferred embodiment of the invention, which proceeds with reference to the accompanying drawings.

BRIEF DESCRIPTION OF THE DRAWINGS

FIG. 1 is graph comparing a conventional encoded bit stream with an encoded bit with rate-distortion optimization according to the invention.

FIG. 2 is a table showing a bit array after transformation.

5 FIG. 3a is a table showing a coding order of a prior art conventional coder.

FIG. 3b is a table showing a coding order of a prior art embedded coder.

FIG. 3c is a table showing a coding order for a rate-distortion optimized embedded coder (RDE) according to the invention.

10 FIG. 4 is a table showing RDE estimation of the rate-distortion slopes based on previously encoded bits.

FIG. 5 is a block diagram of a RDE coder according to the invention.

FIG. 6 is a table showing significance identification bits, refinement bits and sign bits.

FIG. 7 shows an image context for a prior art QM-coder.

15 FIG. 8 is a graph illustrating coding interval subdivisions used for predicting rate-distortion slopes in the RDE coder.

FIG. 9 is a graph showing a rate-distortion slope modification factor for significance identification.

20 FIG. 10 is a flow chart showing how the RDE coder in FIG. 5 performs rate-distortion optimized embedded coding according to the invention.

FIG. 11 is a graph comparing RDE rate-distortion with other encoding techniques.

FIG. 12 is table showing another example of a coding order for the RDE coder.

FIG. 13 is a table comparing rate-distortion for the different encoding techniques in FIG. 11.

25 DETAILED DESCRIPTION

To achieve optimal rate-distortion performance at every truncation point in a bit stream, symbols are encoded in order of their steepest rate-distortion (R-D) slope. The result of the RDE encoder is illustrated in FIG. 1. There are five symbols a, b, c, d and e that are to be coded independently. The coding of each symbol requires a certain amount of bits represented by horizontal rate axis R. Encoding bits result in a certain amount of distortion decrease represented by vertical distortion axis D. Conventional sequential

30

coding in the order of symbol a to e gives the R-D curve shown as solid line 12. The R-D curve shown as dashed line 14 shows the effects when coding is reordered so that the symbol with the steepest R-D slope is encoded first. Though both performance curves reach the same final R-D point, the coder generating the dashed line 14 performs much better when the output bitstream is truncated at any intermediate bit rate.

The rate-distortion optimized coder (RDE) according to the invention, allocates the available coding bits first to the coefficient with the steepest R-D slope. The steepest R-D slope is defined as the coefficient bit that provides the largest distortion decrease in the image per coding bit. When all symbols have been coded, the coding is lossless and RDE may generate similar performance as non-RDE coding techniques. However, RDE optimization outperforms conventional embedded coding at intermediate bit rates. If the filter or transform used to encode image data is not integer based, RDE always outperforms convention embedding since lossless coding can not be achieved.

The two primarily steps performed in RDE are R-D slope calculation and coefficient selection. To avoid sending the overhead of coding order, RDE can be based on an expected R-D slope that is calculated independently by both an encoder and a decoder. The expected R-D slope can be calculated using a lookup table operation in conjunction with a probability estimation table of a QM-coder. Operation of QM-coders are described in W. Pennebaker and J. Mitchell, IBM, "Probability adaptation for arithmetic coders", U.S. Patent No. 5,099,440, Mar. 24, 1992; and D. Duttweiler and C. Chamzas, "Probability estimation in arithmetic and adaptive Huffman entropy coders", IEEE Trans. On Image Processing, vol. 4 no. 3, Mar. 1995, pp. 237-246, which are both herein incorporated by reference.

Implementation of Rate-Distortion Optimized Embedding (RDE)

In the discussion below, it is assumed that an image has already been converted into the transform domain. Any transform can be used with the embedded coding technique including a wavelet decomposition or DCT transform. For simplicity, the RDE is described in terms of a wavelet decomposition. The index of a transform coefficient is denoted by $i=(s,d,x,y)$, where s is a scale of the wavelet decomposition, d is a subband of decomposition which includes LL, LH, HL and HH, and x, y are spatial positions within the subband.

The first and second letter in d represent the filter applied in the vertical and horizontal direction, respectively. The letter L represents a low-pass filter, and H represents a high-pass filter. N denotes the total number of transform coefficients. The coefficient at index position i is denoted by w_i . Assume the coefficients have already been normalized through the division of the maximum absolute value of the transform coefficients T_0 :

$$w'_i = \frac{w_i}{T_0} \quad \text{with} \quad T_0 = \max_i |w_i| \quad (1)$$

To simplify the notation, the apostrophe in w'_i is eliminated and the normalized transform coefficients are simply denoted as w_i . Because w_i is between -1 and $+1$, it can be represented by a stream of binary bits as:

$$\pm 0.b_1 b_2 b_3 \cdots b_j \cdots \quad (2)$$

where b_j is the j -th most significant bit, or alternatively referred to as the j -th coding layer of coefficient w_i . For simplicity, the rate-distortion optimized embedding (RDE) discussion below, the coding symbol is defined as the smallest unit sent to the entropy coder and is either one single bit b_j of the coefficient w_i or the sign of w_i . However, the scope of the invention can easily extended to encoding arrangements, where the coding symbol may consist of encoding a group of bits from each coefficient at the same time, as in the case of the embedded zerotree wavelet coding (EZW) or the set partitioning in hierarchical trees (SPIHT).

A sample bit array produced by a 1D-wavelet transform is shown in FIG. 2. The i -th row of the bit array represents the transform coefficient w_i , and the j -th column of the bit array represents the bit plane b_j . The most significant bit is located at the left most column and the least significant bit is located at the right most column.

The encoding order of the bit-array is different for conventional, embedded, and rate-distortion optimized embedded coders. A conventional coder such as a JPEG coder or a MPEG coder first determines the quantization precision, or equivalently, the number of bits to encode each coefficient, then sequentially encodes one coefficient after another with certain entropy coding. Using the bit array of FIG. 2 as an example, the conven-

tional coding is ordered row by row as further shown in FIG. 3a. A first row 16 is encoded, then a second row 18 is encoded and so on until the entire bit plane is encoded.

Embedded coding is different from the conventional coding shown in FIG. 3a because the image is coded bit-plane by bit-plane (column by column) as shown in FIG. 3b.

The first bit of each coefficient in a first column 20 is encoded starting from the first bit in coefficient w_0 and ending with the first bit in coefficient w_7 . The embedded coder then starts encoding a second column 22 of coefficients starting from the second bit of coefficient w_0 and ending with the second bit of coefficient w_7 . The embedded bitstream can be truncated and still maintain some image quality since the most significant part of each coefficient is coded first. It is also suited for progressive image transmission because the quality of the decoded image gradually improves as more and more bits are received. On the other hand, the coding order of the embedded coding technique shown in FIG. 3b is not optimized for progressive image transmission.

RDE calculates the R-D slope λ_i for each bit b_j and encodes the bit with the largest R-D slope. The actual coding order of RDE depends on the calculated R-D slope and is image dependent. An example of the coding order of RDE is shown in FIG. 3c where a first group of bits 24 shown in cross-hatching comprising the first bits of coefficients w_0 through w_4 are encoded first and then a second group of bits 26 shown in opposite cross-hatching are encoded next. The order of encoding in the second group of bits 26 begins by encoding the second bit of coefficient w_0 , then the second bit of coefficients w_2 and then coefficient w_3 . Finally the first bits of coefficients w_4 through w_7 are encoded. The same process is conducted for the checkered bits in group 28 starting with the second bit of coefficient w_1 and ending with the second bit of coefficient w_7 . The process is continued until a specified bit rate is reached or all coefficients are encoded. Another more elaborated coding order of RDE is shown in table 1 of FIG. 12. The order of coding, the symbol to encode and its value are listed in column 1, 2 and 3, respectively.

Expected Rate-Distortion Slope

If the optimization is based on the actual rate-distortion (R-D) slope, the decoder has to be informed of the order of coding. A large bit overhead is required to transmit the location of the symbol with the largest actual R-D slope and can easily nullify any advantages that can be brought up by rate-distortion optimization. To avoid transmitting the

coding order, a prediction technique is used to calculate an estimated R-D slope in both the encoder and the decoder.

FIG. 4 shows how the rate-distortion slope is estimated based on the transmitted bits. The bits marked by horizontal hatching have already been coded. The bits marked with a checkered pattern are the next candidate bits for encoding. The letter S indicates the R-D slope for the bit will be estimated using a significance identification mode. The letter R indicates the R-D slope for the bit will be estimated using a refinement estimation mode.

Suppose at a certain coding instance, the most significant (n_i-1) bits of coefficient w_i have been encoded. The next set of candidate bits under consideration is the n_i -th bit of w_i , $i=1, \dots, N$. RDE calculates the expected R-D slope λ_i for each candidate bit b_{n_i} , and encodes the one bit with the largest λ_i value. The expected R-D slope λ_i is based on the coding layer n_i , the significance status of coefficient w_i (whether all of the previous (n_i-1) bits of w_i are zero), and the significance status of its surrounding coefficients.

RDE estimates the distortion decrease per coding bit if bit b_{n_i} is coded. Since the information used to calculate the expected R-D slope can be derived independently by the decoder from the previously transmitted bits, the decoder can follow the coding order of the encoder without any overhead transmission. RDE encodes the symbol that gives the maximum expected distortion decrease per bit spent, thus achieving optimized R-D embedded coding performance as shown by the dashed line 14 in FIG. 1.

An encoder 30 utilizing the RDE coder is shown in FIG. 5. Digitized images 31 are converted into coefficients by a transform 32. The RDE coder comprises a R-D slope calculator 34 that estimates the R-D slopes for the coefficient bits and a symbol selector 36 that selects bits for subsequent encoding according to the calculated R-D slope values. A quantizer 38 quantizes the RDE ordered bits and an arithmetic coder 40 further encodes the quantized bits. The output of quantizer 38 is inverse quantized and subtracted from the coefficient values output from transform 32.

Compared with traditional embedded coders, there are two key operations in RDE, R-D slope calculation and coefficient selection. Both operations have to be efficient so that the computational complexity of RDE remains low.

Calculation of the Rate-Distortion Slope

The coding technique described below allows the expected R-D slope to be derived using a lookup table operation. In RDE, the coding of candidate bits b_{n_i} is encoded using
 5 either a significance identification mode or a refinement mode. If all previously coded bits in coefficient w_i are 0s, $b_j=0$ for $j=1 \dots n_i-1$, the significance identification mode is used to encode bit b_{n_i} ; otherwise, the refinement mode is used. For convenience, coefficient w_i is called insignificant if all its previously coded bits are 0s. The insignificant coefficient is reconstructed with value 0 at the decoder side. When the first nonzero bit b_{n_i} is encoun-
 10 tered, coefficient w_i becomes significant. The sign for the coefficient needs to be encoded to distinguish the coefficient value between positive and negative, and it becomes non-zero at the decoder. From that point on, the refinement mode is used to encode the remaining bits of coefficient w_i .

Referring to FIG. 6, bits encoded during the significant identification mode are
 15 marked with horizontal hatching and bits encoded during the refinement mode are marked with dots. The bits marked by checkerboard patterns are sign bits, which are encoded when a coefficient just becomes significant. The expected R-D slopes and coding methods for significance identification and refinement are different.

In significance identification, the coded bit is highly biased toward '0', i.e., non-
 20 significance. The result of significance identification is encoded with a QM-coder, which estimates the probability of significance of coefficient w_i (denoted as p_i) with a state machine, and then arithmetic encodes it. As shown in FIG. 7, a context of 7 bits is used, which consists of 6 bits 44 shown in light shading representing the significant status for 6 spatial neighbor coefficients and 1 bit 44 shown in dark shading representing the
 25 significant status of the coefficient which corresponds to the same spatial position but one scale up (i.e., in the lower resolution band of) the current coefficient w_i . By monitoring the pattern of past 0s ('insignificance') and 1s ('significance') under the same context (i.e., the same neighborhood configuration), the QM-coder estimates the probability of significance p_i of the current symbol being analyzed. To explain further, if there were n_0 0 sym-

bols and n_1 1 symbols in the past coding with the same context, the probability p that the current symbol appears 1 can be calculated by Bayesian estimation as:

$$p = \frac{n_1 + \delta}{n_0 + \delta + n_1 + \delta} \quad (3)$$

where δ is a parameter between $[0,1]$ which relates to the a priori probability of the coded symbol. The probability p is associated with a state. Depending on whether the coded symbol is 1 or 0, it increases or decreases the probability p and thus transfers the coder to another state. By merging of the state of similar probabilities and balancing between the accuracy of probability estimation and quick response to the change in source characteristics, a QM-coder state table can be designed.

The QM-coder and its probability estimation, are described in W. Pennebaker and J. Mitchell, IBM, "Probability adaptation for arithmetic coders", US patent 5,099,440, Mar. 24, 1992; D. Duttweiler and C. Chamzas, "Probability estimation in arithmetic and adaptive Huffman entropy coders", IEEE Trans. On Image Processing, vol. 4 no. 3, Mar. 1995, pp. 237-246; and W. B. Pennebaker and J. L. Mitchell, "JPEG still image data compression standard", New York: Van Nostrand Reinhold, 1993.

In general, the probability estimation is a table transition operation. The estimated probability of significance p_i is used not only for arithmetic coding, but also for the calculation of the R-D slope λ_i . On the other hand, the refinement and sign bits are equilibrium between '0' and '1'. An arithmetic coder encodes them with fixed probability 0.5.

RDE calculates the expected R-D slope λ_i for all the candidate bits b_{n_i} , which is the average distortion decrease divided by the average coding rate increase:

$$\lambda_i = \frac{E[\Delta D_i]}{E[\Delta R_i]} \quad (4)$$

The expected R-D slope can not be calculated by averaging the distortion decrease per coding rate:

$$\lambda_i \neq E \left[\frac{\Delta D_i}{\Delta R_i} \right] \quad (5)$$

It is just like the calculation of the average speed of a vehicle traveling through different segments with varying speed. Its average speed is equal to the total travel distance divided by the total travel time, not the average of speed of different segments.

5 Referring to FIG. 8, suppose before coding bit b_{n_i} , coefficient w_i is known to be within interval $(M_{0,b}, M_{1,b})$ with decoding reconstruction r_b . Coding of bit b_{n_i} supplies additional information of coefficient w_i and restricts it into one of K subintervals $(M_{k,a}, M_{k+1,a})$ with decoding reconstruction $r_{k,a}$, $k=0, \dots, K-1$. The interval boundaries satisfy the relationship:

$$10 \quad M_{0,b} = M_{0,a} < M_{1,a} < \dots < M_{K,a} = M_{1,b} \quad (6)$$

Whereas the decoding reconstruction is usually at the center of the interval:

$$r_b = (M_{0,b} + M_{1,b})/2, \quad (7)$$

$$\text{and } r_{k,a} = (M_{k,a} + M_{k+1,a})/2, \quad k=0, \dots, K-1. \quad (8)$$

The average distortion decrease and the average coding rate increase are calculated as:

$$15 \quad \sum_{k=0}^{K-1} \int_{M_{k,a}}^{M_{k+1,a}} [(x-r_b)^2 - (x-r_{k,a})^2] p(x) dx, \quad (9)$$

$$\text{and } E[\Delta R_i] = \sum_{k=0}^{K-1} -P_k \log_2 P_k \quad \text{with} \quad P_k = \int_{M_{k,a}}^{M_{k+1,a}} p(x) dx, \quad (10)$$

where $p(x)$ is the a priori probability distribution of the coding symbol which is normalized so that the probability of the entire interval $(M_{0,b}, M_{1,b})$ is equal to 1:

$$\int_{M_{0,b}}^{M_{1,b}} p(x) dx = 1 \quad (11)$$

20 In the case the candidate bit b_{n_i} undergoes significance identification, coefficient w_i is insignificant within interval $(-2T_{n_i}, 2T_{n_i})$ before the coding of b_{n_i} , where $T_{n_i} = 2^{-n_i}$ is the quantization step size determined by the coding layer n_i . After the coding of b_{n_i} , coef-

efficient w_i may be negatively significant with interval $(-2T_{n_i}, -T_{n_i}]$, positively significant with interval $[T_{n_i}, 2T_{n_i})$, or still insignificant with interval $(-T_{n_i}, T_{n_i})$. Thus there are three possible segments after significance identification with segment boundaries:

$$M_{0,b} = M_{0,a} = -2T_{n_i}, \quad M_{1,a} = -T_{n_i}, \quad M_{2,a} = T_{n_i}, \quad \text{and} \quad M_{3,a} = M_{1,b} = 2T_{n_i}, \quad (12)$$

5 The decoding reconstruction value before significance identification is:

$$r_b = 0 \quad (13)$$

The decoding reconstruction values of each segment after significance identification are:

$$r_{0,a} = -1.5T_{n_i}, \quad r_{1,a} = 0, \quad r_{2,a} = 1.5T_{n_i}, \quad \text{respectively.} \quad (14)$$

Because the probability of significance p_i , i.e. the probability $b_{n_i} = 1$ which is esti-

10 mated by the QM-coder, can be formulated as:

$$p_i = \int_{-2T_{n_i}}^{-T_{n_i}} p(x) dx + \int_{T_{n_i}}^{2T_{n_i}} p(x) dx. \quad (15)$$

Assuming that the a priori probability distribution within the significance interval is uniform, $p(x)$ is formulated as:

$$p(x) = \frac{p_i}{2T_{n_i}}, \quad \text{for } T_{n_i} < |x| < 2T_{n_i} \quad (16)$$

15 By substituting equations (12), (13), (14) and (16) into (9) and (10), the average distortion decrease and average coding rate increase are calculated for significance identification as:

$$E[\Delta D_i] = p_i 2.25T_{n_i}^2 \quad (17)$$

$$E[\Delta R_i] = (1-p_i)[- \log_2(1-p_i)] + 2 \frac{p_i}{2} (-\log_2 \frac{p_i}{2}) = p_i + H(p_i) \quad (18)$$

20 where $H(p)$ is the entropy of a binary symbol with probability of 1 equal to p :

$$H(p) = -p \log_2 p - (1-p) \log_2 (1-p) \quad (19)$$

Note that the average distortion (17) is not related to the a priori probability within insignificance interval $(-T_{n_i}, T_{n_i})$, because within that interval the decoding values before

and after coding are both 0. The expected R-D slope for significant identification is derived from (17) and (18) as:

$$\lambda_{i,\text{sig}} = \frac{E[\Delta D_i]}{E[\Delta R_i]} = \frac{2.25 T_{n_i}^2}{1 + H(p_i)/p_i} = f_s(p_i) T_{n_i}^2 \quad (20)$$

Function $f_s(p)$ is the significance R-D slope modification factor defined as:

$$f_s(p) = \frac{2.25}{1 + \frac{H(p)}{p}}, \quad (21)$$

FIG. 9 plots the R-D slope modification factor for significance identification. The symbol with higher probability of significance has a larger R-D slope and is thus favored to be coded first. The calculation of the R-D slope is only based on the coding layer n_i and the probability of significance p_i , which is in turn estimated through the QM-coder state.

The expected R-D slope for refinement coding is similarly derived, where coefficient w_i is refined from interval $[S_i, S_i + 2T_{n_i})$ to one of the two segments $[S_i, S_i + T_{n_i})$ or $[S_i + T_{n_i}, S_i + 2T_{n_i})$. $T_{n_i} = 2^{-n_i}$ is again the quantization step size determined by the coding layer n_i , and S_i is the start of the refinement interval which is determined by the previously coded bits of coefficient w_i . The segment boundaries are:

$$M_{0,b} = M_{0,a} = S_i, \quad M_{1,a} = S_i + T_{n_i}, \quad \text{and} \quad M_{2,a} = M_{1,b} = S_i + 2T_{n_i}, \quad (22)$$

and the corresponding decoding reconstruction values are:

$$r_b = S_i + T_{n_i}, \quad r_{0,a} = S_i + 0.5T_{n_i}, \quad \text{and} \quad r_{1,a} = S_i + 1.5T_{n_i}. \quad (23)$$

Assuming that the a priori probability distribution within interval $[S_i, S_i + 2T_{n_i})$ is uniform, we have:

$$p(x) = \frac{1}{2T_{n_i}}, \quad \text{for } S_i < x < S_i + 2T_{n_i}, \quad (24)$$

The average distortion decrease and coding rate increase for refinement coding are calculated as:

$$E[\Delta D_i] = 0.25 T_{n_i}^2 \quad (25)$$

$$E[\Delta R_i] = 1 \quad (26)$$

The expected R-D slope for refinement coding is thus:

$$\lambda_{i,\text{ref}} = \frac{E[\Delta D_i]}{E[\Delta R_i]} = 0.25 T_{n_i}^2 \quad (27)$$

Comparing (20) and (27), it is apparent that for the same coding layer n_i , the R-D slope of refinement coding is smaller than that of significance identification whenever the significance probability p_i is above 0.01. Thus in general the significance identification coding should be conducted before the refinement coding.

The a priori probability distribution of coefficient w_i can also be modeled with a Laplacian distribution. In this case, the R-D slope for significance identification and refinement becomes:

$$\lambda_{i,\text{sig}} = f_s(p_i) g_{\text{sig}}(s, T_{n_i}) T_{n_i}^2 \quad (28)$$

$$\lambda_{i,\text{ref}} = 0.25 g_{\text{ref}}(s, T_{n_i}) T_{n_i}^2 \quad (29)$$

where σ is the variance of Laplacian distribution that can also be estimated from the already coded coefficients, $g_{\text{sig}}(\sigma, T)$ and $g_{\text{ref}}(\sigma, T)$ are Laplacian modification factors in the form:

$$g_{\text{sig}}(\sigma, T) = \frac{1}{2.25} \left(0.75 + \frac{3\sigma}{T} - \frac{3e^{-T/\sigma}}{1 - e^{-T/\sigma}} \right) \quad (30)$$

$$g_{\text{ref}}(\sigma, T) = 4 \left(0.75 + \frac{\frac{2\sigma}{T} e^{-T/\sigma} - \frac{\sigma}{T} (1 + e^{-2T/\sigma})}{1 - e^{-2T/\sigma}} \right) \quad (31)$$

However, experiments show that the additional performance improvement provided by the Laplacian probability model is minor. Since the uniform probability model is much simpler to implement, it is used throughout the experiments described below.

Because the probability of significance p_i is discretely determined by the QM-coder state, and the quantization step size T_{n_i} associated with the coding layer n_i is also discrete, both the R-D slope of significance identification (20) and refinement (27) have a discrete number of states. For fast calculation, (20) and (27) are pre-computed and stored in a table indexed by the coding layer n_i and the QM-coder state. Computation of the R-D slope is thus a lookup table operation. The R-D slope of refinement needs one entry per

coding layer. The R-D slope of significance identification needs two entries per coding layer and per QM-coder state, as each QM-coder state may correspond to the probability of significance p_i (if the most probable symbol is 1) or the probability of insignificance $1 - p_i$ (if the most probable symbol is 0). Therefore, the total number of entries M in the

5 lookup table is:

$$M=2KL+K \quad (32)$$

where K is the maximum coding layer, L is the number of states in the QM-coder. In the current implementation, there are a total of 113 states in the QM-coder, and a maximum of 20 coding layers. This brings up a lookup table of size 4540 entries.

10 Coefficient Selection

The second RDE step performed by symbol selector 36 in FIG. 5 is selecting the coefficient with the maximum expected R-D slope. This may be done by exhaustive searching or sorting over all candidate bits, which is computationally expensive. An alternative implementation uses a threshold-based approach. The concept is to setup a series of

15 decreasing R-D slope thresholds $\gamma_0 > \gamma_1 > \dots > \gamma_n > \dots$, and to scan the whole image repeatedly. The symbols with R-D slope between γ_n and γ_{n+1} are encoded at iteration n .

The threshold based rate-distortion optimization sacrifices a little bit performance as symbols with R-D slope between γ_n and γ_{n+1} can not be distinguished. However, the coding speed is much faster as the search for the maximum R-D slope is avoided.

20 The entire coding operation of RDE is shown in FIG. 10. The left half of FIG. 10 shows the main RDE operation flow and the right half is a detailed description of R-D slope calculations and symbol coding. Since the symbols of significance identification and refinement are treated differently, they are depicted with separate branches in R-D slope calculation and symbol coding.

25 1) Initialization

The image is decomposed by a transform, such as the wavelet transform, in step 52. An initial R-D slope threshold γ is set to γ_0 in block 54, with:

$$\gamma_0 = \frac{1}{16} T_0^2 \quad (33)$$

2) Scanning

The entire image is scanned in step 56 top-down from the coarsest scale to the finest scale. Scale is defined as resolution of the wavelet decomposition. Within each scale, subbands are coded sequentially with order LL, LH, HL and HH. The coder follows the
5 raster line order within the subband.

3) Calculation of the expected R-D slope

The expected R-D slope is calculated for the candidate bit of each coefficient in blocks 66 and 68. Decision block 64 determines whether the coefficient is significant (whether a binary 1 has yet occurred in the string of coefficient bits). The expected R-D slope is
10 calculated according to equation (20) in block 66 for the significance mode or equation (27) in block 68 for the refinement mode. The calculation of the R-D slope is typically a lookup table operation indexed by the QM-coder state and the coding layer n_i .

4) Coding decision

The calculated R-D slope is compared with the current threshold γ in decision block 70.
15 If the R-D slope is smaller than γ for the current iteration, the RDE coder processes the next coefficient by jumping back to decision block 64. Only the candidate bits with R-D slope greater than γ are encoded.

5) Coding of the candidate bit

Depending again on whether the coefficient is already significant, the candidate bit
20 is coded with significance identification in block 74 or with refinement in block 76. The QM-coder with context designated in FIG. 7 is used for significance identification coding in block 74. A fixed probability arithmetic coder is used to encode the sign and refinement in block 76. The sign bit is encoded right after the coefficient becomes significant. As mentioned above, the QM-coding and arithmetic coding are well known to those skilled in
25 the art and are therefore not described in further detail.

6) Iteration

After the entire image has been scanned, the R-D slope threshold is reduced in block 66 by a factor of α :

$$\gamma \leftarrow \gamma / \alpha \quad (34)$$

In the current implementation, α is set to 1.25. The RDE coder checks if the assigned coding rate is reached in decision block 62. For example, the RDE coder determines if the compressed image has reached a predetermined number of bits. If the coding rate is not reached, the RDE coder jumps back to block 56 and encoding repeated for the remaining unencoded bits at the new lower threshold value.

EXPERIMENTAL RESULTS

Extensive experiments were performed to compare RDE with other existing algorithms. Test images were identified as Lena, Boats, Gold and Barbara. The image Lena is of size 512x512, all other images are of size 720x576. The test image is decomposed by a 5-level 9-7 tap biorthogonal Daubechies filter. It is then compressed by the layered zero coding LZC, proposed by Taubman and Zakhor, the set partitioning in hierarchical trees, as SPIHT proposed by Said and Pearlman, and the rate-distortion optimized embedding (RDE), respectively. The SPIHT coder is used as a reference coder. RDE essentially shuffles the bitstream of LZC and improves its embedding performance. Therefore RDE is compared with LZC to show the advantage of rate-distortion optimization. The initial probability of QM-coder in RDE is set at equilibrium, (i.e., the probabilities of 1 of all contexts are equal to 0.5). No pre- statistics of image is used. The compression ratio in the experiment is chosen to be 8:1 (1.0 bits per pixel (bpp)), 16:1 (0.5bpp), 32:1 (0.25bpp) and 64:1 (0.125bpp). Since all three coders are embedded coders, the coding can be stopped at the exact bit rate.

The comparison results are shown in Table 2 of FIG. 13. The coding rate in bits per pixel is shown in column 2, the peak signal-to-noise ratio (PSNR) of LZC and SPIHT are shown in columns 3 and 4, and the PSNR of RDE and its gain over LZC and SPIHT are shown in column 5, 6 and 7, respectively. The R-D performance curve of the Barbara image is plotted in FIG. 11. The R-D curve of RDE is bold line 78, LZC is represented by solid line 80 and SPIHT is represented by dotted line 82. The R-D curve in FIG. 11 calculates one PSNR point every increment of a few bytes and indicates that RDE outperforms both LZC and SPIHT. The performance gain of RDE over LZC ranges from 0.1 to 0.8dB, with an average of 0.3dB. The gain shows the performance advantage of rate-distortion

optimization. From FIG. 11, it can be observed that the R-D performance curve of RDE is also much smoother than that of LZC. The effect is a direct result of rate-distortion optimization. With the embedded bitstream organized by decreasing rate-distortion slope, the slope of the resultant performance curve decreases gradually, resulting in the smooth looking R-D curve of RDE. The performance gain of RDE over SPIHT ranges from -0.1 to 1.0dB, with an average of 0.4dB.

Thus, rate-distortion optimized embedded coder (RDE) improves the performance of embedded coding at every possible truncation point by coding first the symbol with the steepest R-D slope. That is, at each coding instance, RDE spends bits encoding the coding symbol with the largest distortion decrease per coding bit. For synchronisation between the encoder and the decoder, RDE uses the expected R-D slope, which can be calculated independently by both the encoder and the decoder. It also takes advantage of the probability estimation table of the QM-coder so that the calculation of the R-D slope can be performed using a lookup table operation.

Having described and illustrated the principles of the invention in a preferred embodiment thereof, it should be apparent that the invention can be modified in arrangement and detail without departing from such principles. I claim all modifications and variation coming within the spirit and scope of the following claims.

CLAIMS

1. An rate-distortion optimization method for embedded coding of an image,
5 comprising:
digitizing the image;
transforming the image to form a set of coefficients;
quantizing the coefficient to form a set of symbols;
calculating the distortion reduction values for each symbol representing
10 a ratio of information content in the symbol per cost in transmitting the symbol; and
encoding the symbols according to a descending order of distortion reduction
value.
2. A rate-distortion optimization method for embedded coding of an image,
15 comprising:
digitizing the image;
transforming the image to form a set of coefficients each comprising multiple bits;
repeatedly analyzing a group of candidate bits before encoding individual bits, the
candidate bits comprising the most significant unencoded bit from each coefficient;
20 determining distortion-reduction values for the bits among the candidate bits
representing a ratio of information content in the bit per cost in transmitting the bit;
encoding a selected bit among the candidate bits with an entropy coder; and
substituting the coded bit in the candidate bits with the next most significant
unencoded bit of the coefficient.
25
3. A method according to claim 2 wherein encoding selected bits comprises
encoding one bit among the candidate bits having a maximum distortion reduction value
per coding bit spent.
- 30 4. A method according to claim 2 including the following:
setting a threshold value;

encoding the bits among the candidate bits having rate-distortion slope values greater than threshold value;

reducing the threshold value; and

reconfiguring the candidate bits to include the most significant unencoded bits in
5 each coefficient.

5. A method according to claim 2 wherein the distortion reduction value for each bit is derived from a predicted rate-distortion slope.

10 6. A method according to claim 5 wherein the predicted rate-distortion slope is generated according to the coding layer of each bit, a significance status of the coefficient indicating whether all previous bits in the coefficient are zeros, and the significance statuses of surrounding coefficients.

15 7. A method according to claim 5 wherein the predicted rate distortion slope is derived for each bit according to a significance identification mode or a refinement mode.

8. A method according to claim 7 wherein the significance identification mode encodes all significant bits in the coefficients defined as all bits up to a first binary 1 value
20 and the refinement mode encodes all refinement bits defined as all bits after the first binary 1 value.

9. A method according to claim 7 wherein the significance identification mode uses a QM-coder that estimates a probability that the bit is significant according to a
25 significant status of the same and adjacent coefficients.

10. A method according to claim 8 wherein the rate distortion slope is derived for the significant bits as follows:

$$\lambda_{i,\text{sig}} = \frac{E[\Delta D_i]}{E[\Delta R_i]} = \frac{2.25 T_{n_i}^2}{1 + H(p_i)/p_i} = f_s(p_i) T_{n_i}^2,$$

30 where the function $f_s(p)$ is the significance R-D slope modification factor defined as:

$$f_s(p) = \frac{2.25}{1 + \frac{H(p)}{p}},$$

T_{n_i} is a quantization step size determined by the coding layer n_i , p_i is probability of significance that a candidate bit $b_{n_i}=1$, and $H(p)$ is entropy of a binary symbol.

- 5 11. A method according to claim 8 wherein the rate distortion slope derived for the refinement bits is the following:

$$\lambda_{i,\text{ref}} = \frac{E[\Delta D_i]}{E[\Delta R_i]} = 0.25 T_{n_i}^2,$$

where T_{n_i} is a quantization step size determined by the coding layer n_i .

- 10 12. A method according to claim 8 wherein the rate distortion slope for the significance bits and the refinement bits are derived according to a Laplacian probability distribution.

- 15 13. A method according to claim 7 including precomputing and storing a table containing the rate-distortion slope values for significance bit coding and refinement bit coding and indexing the rate-distortion slope values according to the coding layer and a coder state corresponding the probability of significance or insignificance that the most probable bit during the significant identification mode is a 1 or a 0.

- 20 14. An embedded encoder for optimizing rate-distortion coding of a digitized image, comprising:

a transformer encoding the digitized image forming a set of coefficients each comprising multiple bits;

- 25 a rate-distortion slope calculator repeatedly analyzing candidate bits for each coefficient comprising a most significant unencoded bit from each coefficient and

determining individual distortion reduction values for individual bits representing a ratio of information content in the bit per cost in transmitting the bit; and

a symbol selector selecting an order for encoding the bits according to the associated distortion reduction values.

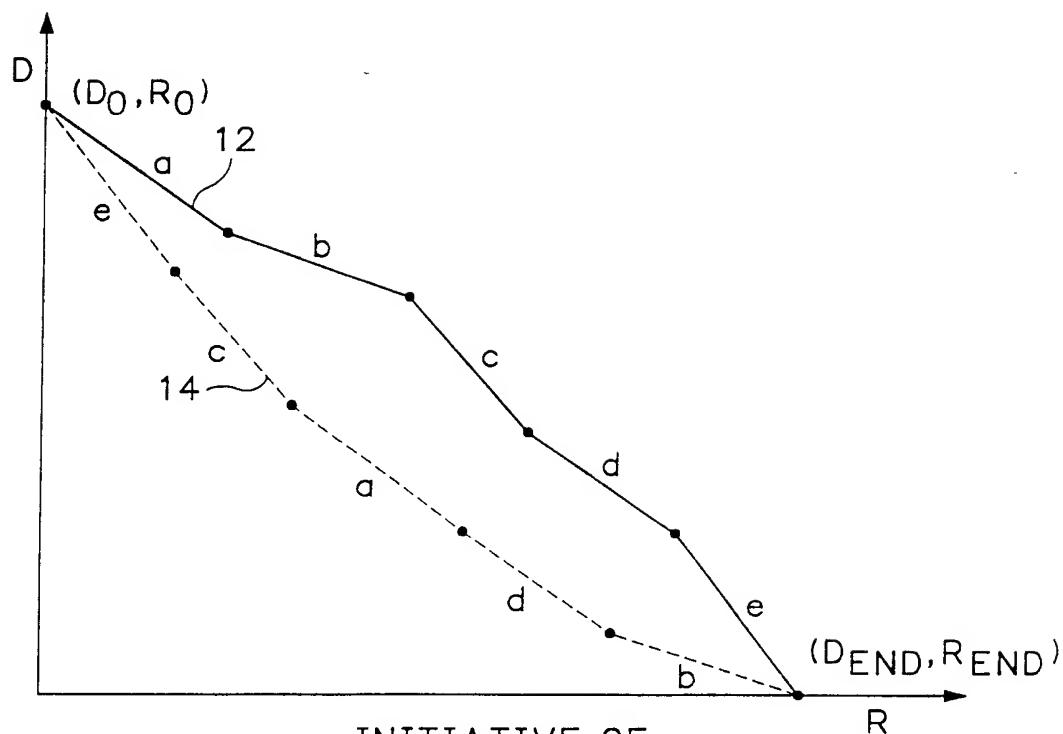
5

15. A system according to claim 14 wherein the rate-distortion slope calculator operates in a significance identification mode when all previously coded bits in the coefficient are zero and a refinement mode after a first nonzero bit is identified in the coefficient during the significance identification mode.

10

16. A system according to claim 15 wherein the rate-distortion slope calculator comprises a lookup table including one refinement mode rate-distortion entry for each layer of coefficient bits and two significance identification mode rate-distortion entries, a first entry for a symbol 1 to be the most probable symbol, and

15 a second entry for a symbol 0 to be the most probable symbol for each one of multiple QM-coder states each associated with a probability of significance.



INITIATIVE OF
RATE-DISTORTION OPTIMIZATION

FIG.1

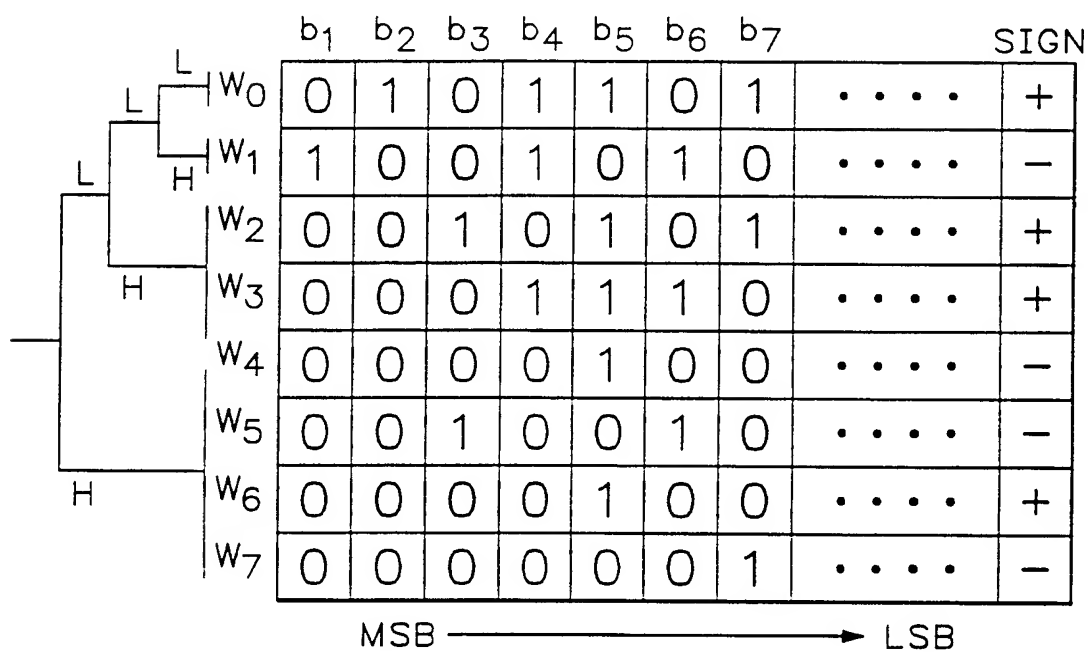


FIG.2

(PRIOR ART)

| | b ₁ | b ₂ | b ₃ | b ₄ | b ₅ | b ₆ | b ₇ | ... | SIGN |
|----------------|----------------|----------------|----------------|----------------|----------------|----------------|----------------|-----|------|
| w ₀ | 0 | 1 | 0 | 1 | 1 | 0 | 1 | ... | + |
| w ₁ | 1 | 0 | 0 | 1 | 0 | 1 | 0 | ... | - |
| w ₂ | 0 | 0 | 1 | 0 | 1 | 0 | 1 | ... | + |
| w ₃ | 0 | 0 | 0 | 1 | 1 | 1 | 0 | ... | + |
| w ₄ | 0 | 0 | 0 | 0 | 1 | 0 | 0 | ... | - |
| w ₅ | 0 | 0 | 1 | 0 | 0 | 1 | 0 | ... | - |
| w ₆ | 0 | 0 | 0 | 0 | 1 | 0 | 0 | ... | + |
| w ₇ | 0 | 0 | 0 | 0 | 0 | 0 | 1 | ... | - |

FIRST ROW 16
 SECOND ROW 18
 THIRD ROW

FIG.3a

| | b ₁ | b ₂ | b ₃ | b ₄ | b ₅ | b ₆ | b ₇ | ... | SIGN |
|----------------|----------------|----------------|----------------|----------------|----------------|----------------|----------------|-----|------|
| w ₀ | 0 | 1 | 0 | 1 | 1 | 0 | 1 | ... | + |
| w ₁ | 1 | 0 | 0 | 1 | 0 | 1 | 0 | ... | - |
| w ₂ | 0 | 0 | 1 | 0 | 1 | 0 | 1 | ... | + |
| w ₃ | 0 | 0 | 0 | 1 | 1 | 1 | 0 | ... | + |
| w ₄ | 0 | 0 | 0 | 0 | 1 | 0 | 0 | ... | - |
| w ₅ | 0 | 0 | 1 | 0 | 0 | 1 | 0 | ... | - |
| w ₆ | 0 | 0 | 0 | 0 | 1 | 0 | 0 | ... | + |
| w ₇ | 0 | 0 | 0 | 0 | 0 | 0 | 1 | ... | - |

20 FIRST COLUMN
 22 SECOND COLUMN
 THIRD COLUMN

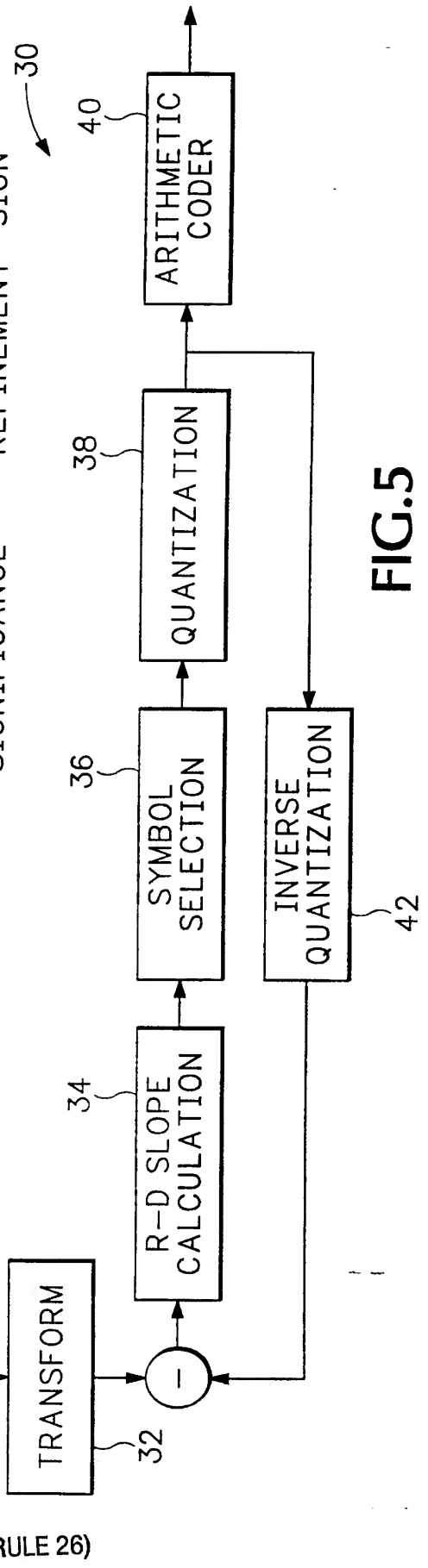
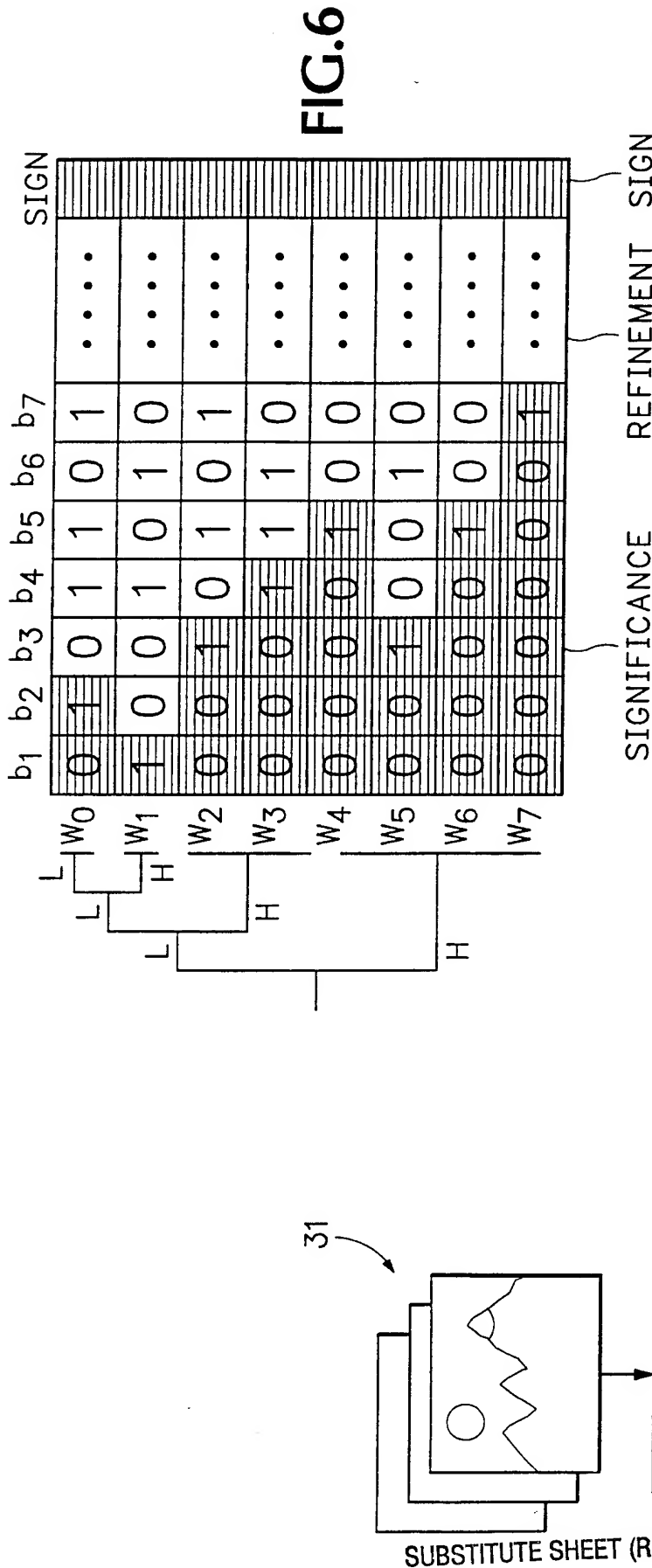
FIG.3b

| | | b ₁ | b ₂ | b ₃ | b ₄ | b ₅ | b ₆ | b ₇ | | SIGN |
|----------------------|----------------|----------------|----------------|----------------|----------------|----------------|----------------|----------------|-----|------|
| FIRST GROUP 24 | w ₀ | 0 | 1 | 0 | 1 | 1 | 0 | 1 | ... | + |
| | w ₁ | 1 | 0 | 0 | 1 | 0 | 1 | 0 | ... | - |
| | w ₂ | 0 | 0 | 1 | 0 | 1 | 0 | 1 | ... | + |
| | w ₃ | 0 | 0 | 0 | 1 | 1 | 1 | 0 | ... | + |
| | w ₄ | 0 | 0 | 0 | 0 | 1 | 0 | 0 | ... | - |
| | w ₅ | 0 | 0 | 1 | 0 | 0 | 1 | 0 | ... | - |
| | w ₆ | 0 | 0 | 0 | 0 | 1 | 0 | 0 | ... | + |
| | w ₇ | 0 | 0 | 0 | 0 | 0 | 0 | 1 | ... | - |

FIG.3c

| | | b ₁ | b ₂ | b ₃ | b ₄ | b ₅ | b ₆ | b ₇ | | SIGN |
|--|----------------|----------------|----------------|----------------|----------------|----------------|----------------|----------------|-----|------|
| | W ₀ | 0 | 1 | 0 | r | 1 | 0 | 1 | ... | + |
| | W ₁ | 1 | 0 | 0 | r | 0 | 1 | 0 | ... | - |
| | W ₂ | 0 | 0 | 1 | r | 1 | 0 | 1 | ... | + |
| | W ₃ | 0 | 0 | 0 | s | 1 | 1 | 0 | ... | + |
| | W ₄ | 0 | 0 | 0 | 0 | s | 0 | 0 | ... | - |
| | W ₅ | 0 | 0 | 1 | r | 0 | 1 | 0 | ... | - |
| | W ₆ | 0 | 0 | 0 | 0 | s | 0 | 0 | ... | + |
| | W ₇ | 0 | 0 | 0 | s | 0 | 0 | 1 | ... | - |

FIG. 4



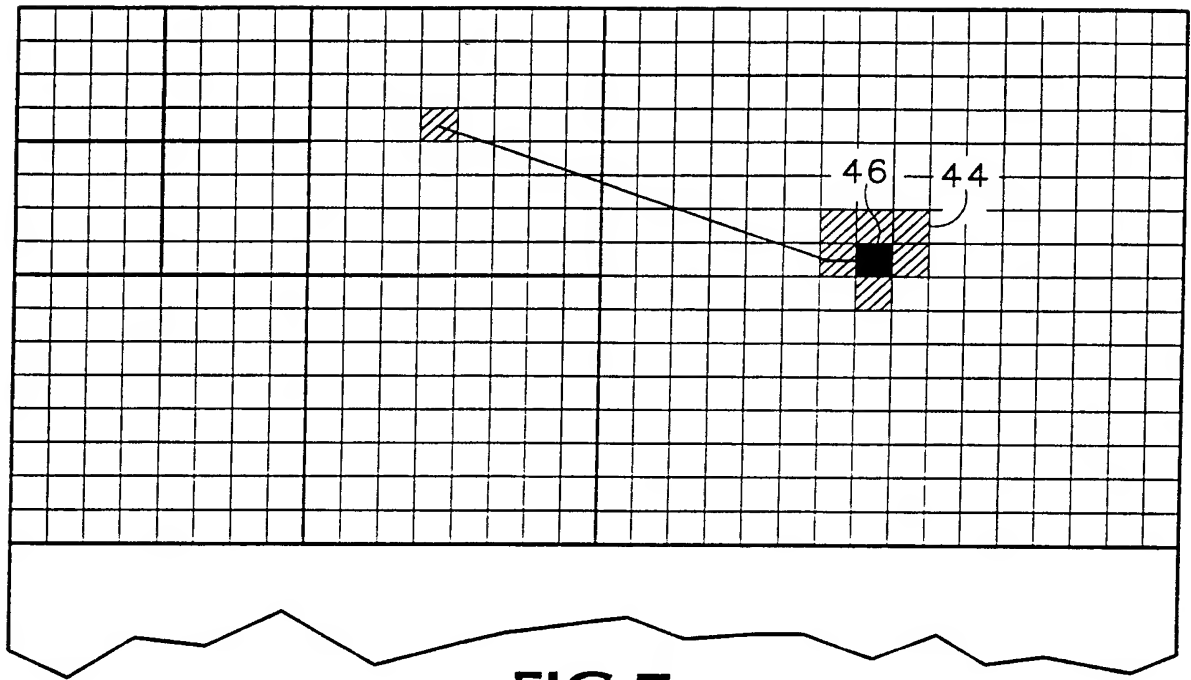


FIG. 7

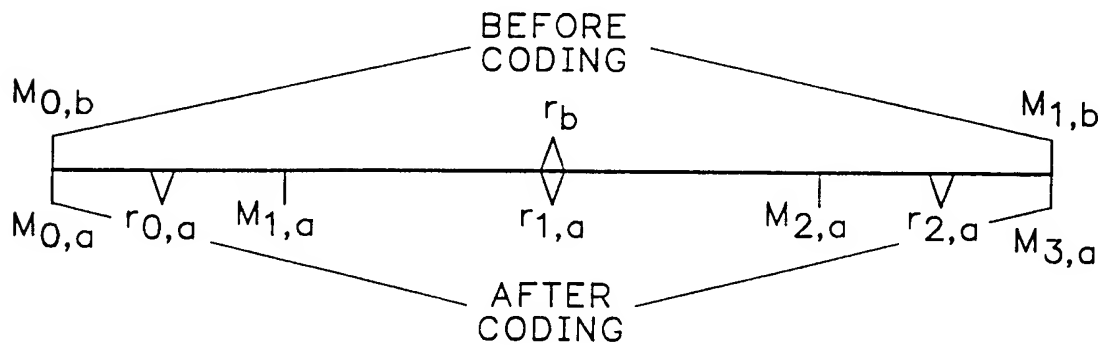
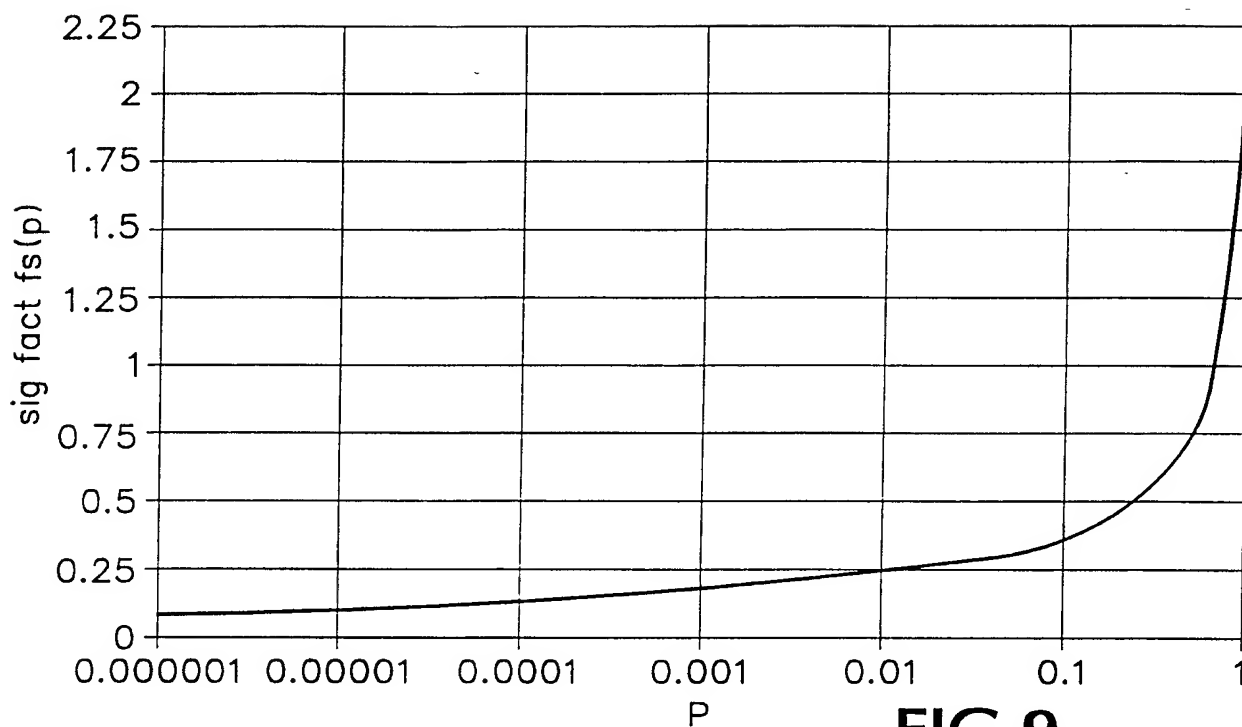
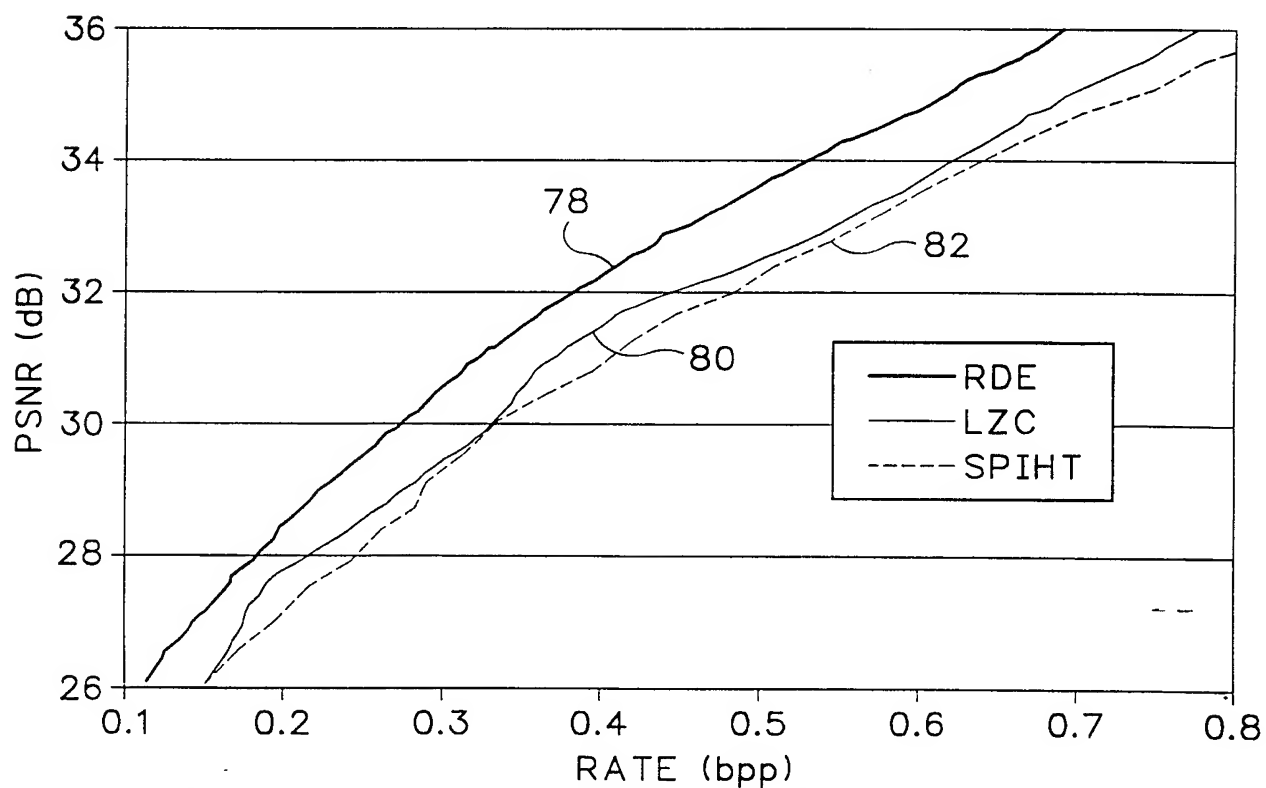


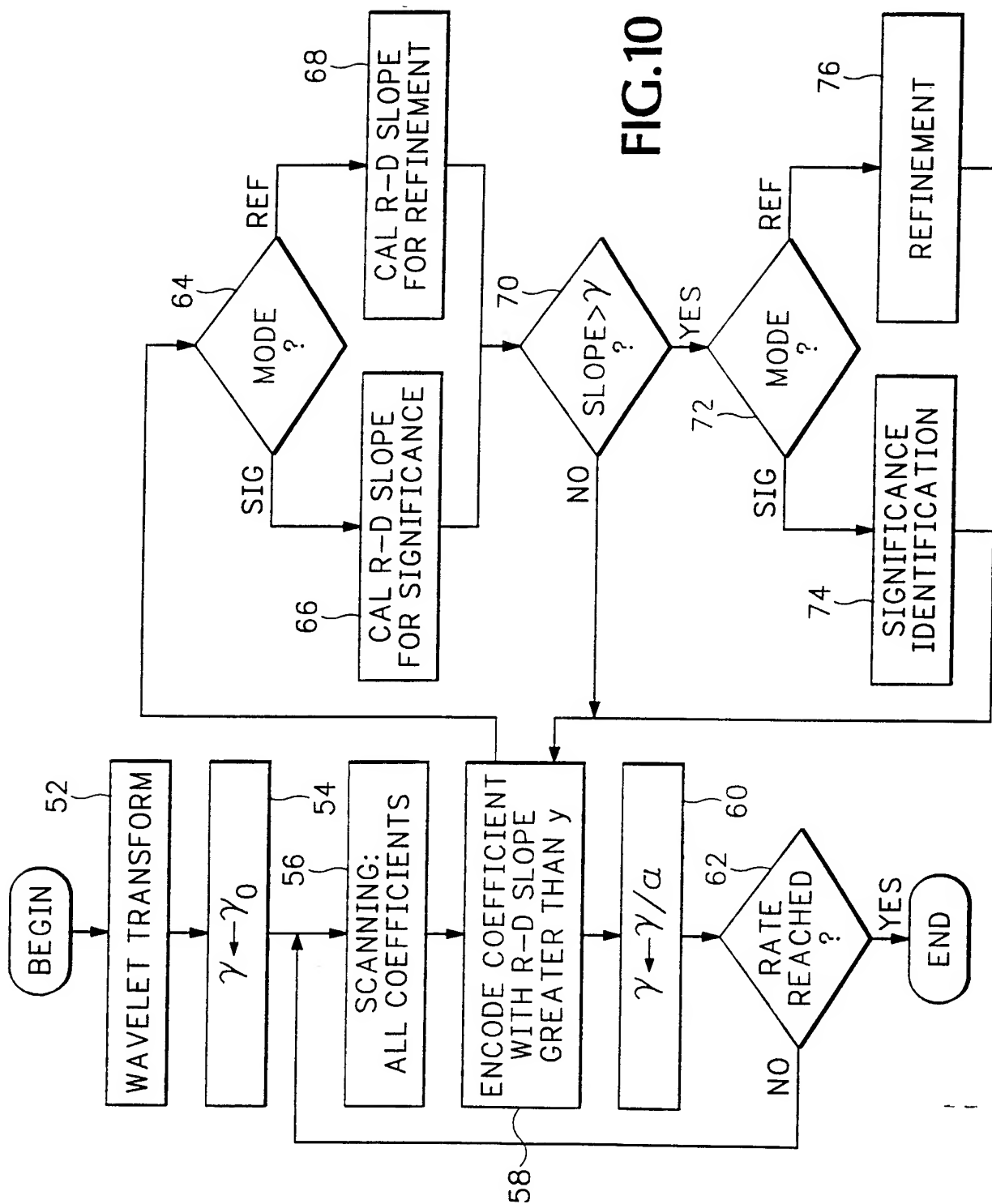
FIG. 8

6 /9

**FIG.9**

RATE-DISTORTION CURVE OF RDE, LZC AND SPIHT

FIG.11



| ORDER | SYMBOL | VALUE | ORDER | SYMBOL | VALUE | ORDER | SYMBOL | VALUE |
|-------|-----------------------|-------|-------|-----------------------|-------|-------|-----------------------|-------|
| 1 | $b_1 \text{ OF } w_0$ | 0 | 10 | $b_1 \text{ OF } w_4$ | 0 | 19 | $b_2 \text{ OF } w_5$ | 0 |
| 2 | $b_1 \text{ OF } w_1$ | 1 | 11 | $b_1 \text{ OF } w_5$ | 0 | 20 | $b_2 \text{ OF } w_6$ | 0 |
| 3 | SIGN OF w_1 | - | 12 | $b_1 \text{ OF } w_6$ | 0 | 21 | $b_2 \text{ OF } w_7$ | 0 |
| 4 | $b_1 \text{ OF } w_2$ | 0 | 13 | $b_1 \text{ OF } w_7$ | 0 | | | |
| 5 | $b_1 \text{ OF } w_3$ | 0 | 14 | $b_2 \text{ OF } w_1$ | 0 | | | |
| 6 | $b_2 \text{ OF } w_0$ | 1 | 15 | $b_3 \text{ OF } w_2$ | 1 | | | |
| 7 | SIGN OF w_0 | + | 16 | SIGN OF w_2 | + | | | |
| 8 | $b_2 \text{ OF } w_2$ | 0 | 17 | $b_3 \text{ OF } w_3$ | 0 | | | |
| 9 | $b_2 \text{ OF } w_3$ | 0 | 18 | $b_2 \text{ OF } w_4$ | 0 | | | |

TABLE 1
FIG.12

| IMAGE | RATE (bpp) | LZC PSNR(dB) | SPIHT PSNR(dB) | PSNR(dB) | RDE GAIN VS LZC(dB) | GAIN VS SPIHT (dB) |
|---------|---------------|-----------------|-------------------|----------|------------------------|--------------------|
| LENA | 1 | 40.1 | 40.4 | 40.3 | 0.2 | -0.1 |
| | 0.5 | 37.1 | 37.2 | 37.2 | 0.1 | 0.0 |
| | 0.25 | 34.1 | 34.1 | 34.2 | 0.1 | 0.1 |
| | 0.125 | 31.1 | 31.1 | 31.3 | 0.2 | 0.2 |
| BARBARA | 1 | 37.5 | 37.6 | 38.1 | 0.6 | 0.5 |
| | 0.5 | 32.6 | 32.3 | 33.1 | 0.5 | 0.8 |
| | 0.25 | 28.6 | 28.2 | 29.1 | 0.5 | 0.9 |
| | 0.125 | 25.3 | 25.1 | 26.1 | 0.8 | 1.0 |
| BOATS | 1 | 41.2 | 41.1 | 41.6 | 0.4 | 0.5 |
| | 0.5 | 36.9 | 36.5 | 37.0 | 0.1 | 0.5 |
| | 0.25 | 33.1 | 32.5 | 33.2 | 0.1 | 0.7 |
| | 0.125 | 29.9 | 29.3 | 30.0 | 0.1 | 0.7 |
| GOLD | 1 | 37.5 | 37.6 | 37.7 | 0.2 | 0.1 |
| | 0.5 | 34.0 | 34.1 | 34.3 | 0.3 | 0.2 |
| | 0.25 | 31.4 | 31.3 | 31.6 | 0.2 | 0.3 |
| | 0.125 | 29.3 | 29.0 | 29.5 | 0.2 | 0.5 |

TABLE 2
FIG.13

INTERNATIONAL SEARCH REPORT

International application No.
PCT/US98/01981

A. CLASSIFICATION OF SUBJECT MATTER

IPC(6) :G06K 9/36, 9/46
US CL :382/239,240,247; 348/398,405,408,419
According to International Patent Classification (IPC) or to both national classification and IPC

B. FIELDS SEARCHED

Minimum documentation searched (classification system followed by classification symbols)

U.S. : 382/239,240,247; 348/398,405,408,419

Documentation searched other than minimum documentation to the extent that such documents are included in the fields searched

Electronic data base consulted during the international search (name of data base and, where practicable, search terms used)
IEEE

C. DOCUMENTS CONSIDERED TO BE RELEVANT

| Category* | Citation of document, with indication, where appropriate, of the relevant passages | Relevant to claim No. |
|---------------|--|----------------------------|
| X --- Y | Said, et al., A New, Fast, and Efficient Image Codec Based on Set Partitioning in Hierarchical Trees. IEEE Transactions on Circuits and Systems for Video Technology, Vol. 6, No. 3, June 1996. Pages 243-250, especially pages 244-24. | 1-3 ----- 4-9, 12-16 |
| Y | Ramchandran et al., Bit Allocation for Dependent Quantization with Applications to Multiresolution and MPEG Video Coders. IEEE Transactions on Image Processing, Vol. 3, No. 5, September 1994. Pages 533-545, especially pages 533-534, 537-539, 541-544. | 4-9, 12-16 |
| Y | US 5,099,440 A (Pennebaker et al.) 24 March 1992 (24.03.92), paragraph bridging cols. 11-12, c. 4, lines 25-54, c. 15, lines 23-27. | 9, 13, 16 |

☒ Further documents are listed in the continuation of Box C. ☐ See patent family annex.

| | |
|---|--|
| * Special categories of cited documents: | "T" later document published after the international filing date or priority date and not in conflict with the application but cited to understand the principle or theory underlying the invention |
| "A" document defining the general state of the art which is not considered to be of particular relevance | "X" document of particular relevance; the claimed invention cannot be considered novel or cannot be considered to involve an inventive step when the document is taken alone |
| "E" earlier document published on or after the international filing date | "Y" document of particular relevance; the claimed invention cannot be considered to involve an inventive step when the document is combined with one or more other such documents, such combination being obvious to a person skilled in the art |
| "L" document which may throw doubts on priority claim(s) or which is cited to establish the publication date of another citation or other special reason (as specified) | "&" document member of the same patent family |
| "O" document referring to an oral disclosure, use, exhibition or other means | |
| "P" document published prior to the international filing date but later than the priority date claimed | |

Date of the actual completion of the international search
12 AUGUST 1998

Date of mailing of the international search report
02 OCT 1998

Name and mailing address of the ISA/US
Commissioner of Patents and Trademarks
Box PCT
Washington, D.C. 20231
Facsimile No. (703) 305-3230

Authorized officer
Amelia Au *Diane Smith for*
Telephone No. (703) 308-6604

INTERNATIONAL SEARCH REPORT

International application No.
PCT/US98/01981

C (Continuation). DOCUMENTS CONSIDERED TO BE RELEVANT

| Category* | Citation of document, with indication, where appropriate, of the relevant passages | Relevant to claim No. |
|-----------|---|-----------------------|
| Y, E | US 5,778,192 A (Schuster et al.) 07 July 1998 (07.07.98), column 10, third full paragraph and paragraph bridging columns 10-11. | 13 |
| Y | US 4,811,398 A (Copperi et al.) 07 March 1989 (07.03.89), column 7, lines 24-28 and column 21, lines 40-45. | 12 |